



NIH Public Access

Author Manuscript

ACS Chem Biol. Author manuscript; available in PMC 2014 November 15.

Published in final edited form as:

ACS Chem Biol. 2013 November 15; 8(11): . doi:10.1021/cb400601g.

Photoreactive “Nanorulers” Detect a Novel Conformation of Full length HDAC3-SMRT Complex in Solution

Hazem Abdelkarim[†], Michael Brunsteiner[†], Raghupathi Neelarapu[†], He Bai[†], Antonett Madriaga[†], Richard B. van Breemen[†], Sylvie Y. Blond[‡], Vadim Gaponenko[‡], and Pavel A. Petukhov^{†,*}

[†] Department of Medicinal Chemistry and Pharmacognosy, College of Pharmacy, University of Illinois at Chicago, 833 South Wood Street, Chicago, IL 60612, USA

[‡]Center for Pharmaceutical Biotechnology, University of Illinois at Chicago, 900 South Ashland, Chicago, IL 60612, USA

[‡]Department of Biochemistry and Molecular Genetics, University of Illinois at Chicago, 900 S Ashland, Chicago, IL 60607, USA.

Abstract

Histone deacetylase 3 (HDAC3) is a promising epigenetic drug target for multiple therapeutic applications. Direct interaction between the Deacetylase Activating Domain of the silencing mediator for retinoid or thyroid hormone receptors (SMRT-DAD) is required for activation of enzymatic activity of HDAC3. The structure of this complex and the nature of interactions with HDAC inhibitors in solution are unknown. Using novel photoreactive HDAC probes – “nanorulers”, we determined the distance between the catalytic site of the full-length HDAC3 and SMRT-DAD in solution at physiologically relevant conditions and found it to be substantially different from that predicted by the X-ray model with a Δ379-428aa truncated HDAC3. Further experiments indicated that in solution this distance might change in response to chemical stimuli, while the enzymatic activity remained unaffected. These observations were further validated by Saturation Transfer Difference (STD) NMR experiments. We propose that the observed changes in the distance are an important part of the histone code that remains to be explored. Mapping direct interactions and distances between macromolecules with such “nanorulers” as a function of cellular events facilitates better understanding of basic biology and ways for its manipulation in cell and tissue specific manner.

Histone deacetylases (HDACs) are a family of enzymes involved in the regulation of gene transcription through deacetylation of lysine side chains in histones and other proteins.⁽¹⁾ HDACs, in particular HDAC3, have emerged as potential drug targets for multiple therapeutic applications.⁽²⁻⁶⁾ The design of selective inhibitors of particular HDAC isoforms is necessary to enhance *in vivo* potency, reduce toxicity of currently available inhibitors, and to broaden the therapeutic scope of HDAC inhibitors.⁽⁷⁻⁹⁾ As most of HDAC isoforms assemble with other proteins to form multiprotein complexes with unique functionalities,⁽¹⁰⁾ the structures of these complexes hold the key for ways to manipulate the epigenetic machinery in tissue/cell-specific manner. In mammalian cells, HDAC3 is found in a large protein complex with the silencing mediator for retinoid or thyroid hormone receptors (SMRT), also referred to as the nuclear receptor co-repressor 2 (NCOR2), GPS2, TBL1, and

* Corresponding author: Phone: 312-996-4174. Fax: 312-996-7107. pap4@uic.edu.

Supporting Information Available: Synthetic and analytical methods for the compounds described herein; detailed description of the activity assay, photolabeling experiments, molecular analysis, and docking calculations; Supplementary Figures S1–S8 and Tables S1 and S2. This material is available free of charge via the Internet at <http://pubs.acs.org>.

TBLR1.⁽¹¹⁾ This complex recruits additional co-repressors/co-activators and binds to nuclear receptors,⁽¹²⁾ resulting in modulation of gene expression. Direct interaction of HDAC3 with the deacetylase activating domain (DAD), a segment of approximately 80 amino acids in the SANT1 domain of SMRT,^(13, 14) is both required and sufficient for HDAC3 activation in vitro and in vivo.^(15, 16) The knowledge of the three-dimensional structure of this complex may not only enable discovery of novel approaches to inhibit the enzymatic activity of the HDAC3-SMRT complex but also gives hints at how HDAC3 may play a deacetylase-independent function in vivo⁽¹⁶⁾ and possibly even be extended to other deacetylase complexes that contain proteins with similar SANT domains. A recent publication by Schwabe et al.⁽¹⁷⁾ has shed light on the structural features and a possible regulatory role of D-myo-inositol-(1,4,5,6)-tetrakisphosphate (Ins(1,4,5,6)P₄) in the HDAC3(Δ 379-428aa truncated)-SMRT-DAD complex. Despite the fact that these and other studies by Schwabe and colleagues^(18, 19) have significantly advanced the understanding of HDAC3-SMRT interactions, much remains to be learned about the way these interactions are achieved. Our initial photolabeling studies of the full length HDAC3 in complex with SMRT-DAD with small molecule photoreactive HDAC inhibitors, similar to those we published for HDAC2 and HDAC8,⁽²⁰⁻²²⁾ have suggested that SMRT is located closer than that in the X-ray model. The limitations associated with the truncation of amino acids 379-428 at the HDAC3 C-terminal,⁽²³⁾ the missing “foot pocket”,⁽²¹⁾ and possible differences in the conformations of the HDAC3-SMRT-DAD complex in crystalline and solution states warranted further studies. Since most widely used methods to study^(24, 25) three-dimensional protein structures and protein-protein interactions in solution^{20, 21} have known limitations,⁽²⁶⁻³⁰⁾ we devise a different approach. Here, we present a study that shows for the first time the use of small molecule photoreactive HDAC probes (“nanorulers”) to characterize the distance between the components in the solution structure of the full-length active form of recombinant and cellular HDAC3-SMRT complex. The findings were then independently validated by saturation transfer difference (STD) NMR experiments.

To facilitate the analysis of the HDAC3-SMRT-DAD complex in solution, we designed a series of novel photoreactive inhibitors/probes (Figure 1). The design of these probes included decoration of HDAC ligands with an arylazide moiety or a 3-azido-5-azidomethylene moiety, a photoaffinity labeling group originally proposed by Suzuki et al.⁽³¹⁾ We recently demonstrated that the diazide moiety can be successfully incorporated as part of highly potent HDAC inhibitors that can be used in photolabeling experiments with different HDAC isoforms.^(21, 22, 32) The probes holding the diazide moieties are capable of crosslinking the protein and reacting with the biotin alkyne tag **9** (Figure 1). The probes **5** and **6** with a monoazide moiety are only capable of crosslinking and cannot result in a biotinylated adduct with HDAC protein and, therefore, are used as competitors for the diazide probes **1-4**, **7**, and **8**. The distance between the hydroxamate group and the terminal aryldiazide moiety in the extended conformation varied between 5 Å to 25 Å for the shortest and the longest probes “nanorulers” **4** and **1**, respectively. To evaluate whether the alkylazido moiety is available for copper catalyzed (3+2) cycloligation, we performed a preliminary docking of the probes to a homology model of HDAC3 (the X-ray of HDAC3-SMRT-DAD was not yet published at that time) using a previously published by us procedure.^(32, 33) The probes were also docked to the X-ray of the HDAC3-SMRT-DAD complex (PDB: 4A69) when it became available in PDB. The poses of the probes were found to be comparable to those we obtained with the X-ray model and very similar to the poses of the hydroxamate-based ligands co-crystallized with HDAC8. The probes appeared to be able to extend the alkylazido moiety beyond the relatively narrow well of the active site.

The synthesis of probes **1**, **6**, biotin tag **9**, and intermediates **10** and **11** was described previously.^(22, 32) Probes **2-5** were synthesized as shown in Scheme 1. Substituted benzoic acids **10**, **11**, and **14**, were chosen as precursors for the synthesis of the photoreactive probes. 3-Azido-5-(azidomethyl) benzoic acid (**11**) and its methyl ester (**10**) were synthesized as reported previously,⁽³²⁾ whereas 4-azidoaniline hydrochloride (**14**) was available commercially. The synthesis of the probes **2-5** proceeded through a carbodiimide based coupling reaction followed by conversion of the resulting ester products into the correspondent hydroxamic acids to give the final probes in a 50-70% overall yield. The synthesis of the probes **7** and **8** proceeded through a direct reductive amination reaction followed by alkylation of the monoalkylated amino ester with tosylate alcohol of the diazide probe. The ester intermediates were then converted to the hydroxamic acids to give the final probes (Supplementary Scheme S1).

The IC₅₀s of the probes for deacetylase activity of the HDAC3-SMRT-DAD complex were determined using a competitive fluorescence-based assay reported by us previously and are provided in Figure 1.⁽³²⁾ The inhibition of HDAC3 was measured using the fluorescent HDAC substrate Boc-L-Lys(Ac)-AMC and commercially available recombinant human HDAC3-SMRT-DAD co-expressed in baculovirus expression system in insect cells. The HDAC3 protein contained a C-terminal His tag and SMRT-DAD protein contained an N-terminal GST tag. The IC₅₀s ranged from double/triple-digit nanomolar for probes **1**, **2**, **5**, **6**, **7**, and **8** to micromolar for probes **3** and **4**.

To study photocrosslinking of the probes **1-8** with the HDAC3-SMRT-DAD complex in solution, we conducted a series of concentration-dependent and competition experiments shown in Figure 2. The diazide probes **1** and **2** gave a dose dependent biotinylation of both HDAC3 and SMRT-DAD (Figure 2a). Incubation of probe **3** and **4** at concentration ranging from 0.85 μM to 34 μM (above the IC₅₀ of probe **3**) with 1.7 μM HDAC3-SMRT-DAD showed only marginally detectable background levels of biotinylation and no increase in biotinylation with either HDAC3 or SMRT-DAD at all the concentrations tested (Figure 2a). We attributed this faint biotinylation by probes **3** and **4** to a non-specific binding of the biotin alkyne tag **9** to proteins similar to that found previously by us and others.^(22, 34, 35) To confirm the specific binding of probes **1** and **2** and only a non-specific biotinylation in the case of probes **3** and **4**, we performed a series of competition experiments with monoazide probes **5** and **6** (Figure 2b). Probe **1** was tested with several concentrations of the competitor - monoazide **6**, whereas probes **2-4** were only tested with one concentration of the competitor – monoazide **5**. For comparison and to validate that the outcome of the competition does not depend on the structure of the monoazide competitor, we included probe **1**, as control on the same gel, and tested probe **2** at two different concentrations (Figure 2b). We observed a dose-dependent increase in biotinylation of the bands of HDAC3 and SMRT-DAD as the concentration of monoazide **6** decreased from 12 μM to 1.2 μM, with the highest intensity of the bands observed in the absence of monoazide **6** (Figure 2b). As with probe **1**, we observed a concentration-dependent increase in biotinylation of HDAC3 and SMRT-DAD as the concentration of probe **2** increased from 1.7 μM to 8.5 μM (Figure 2b). Both probes **1** and **2** show a pronounced difference in biotinylation of HDAC3 and SMRT-DAD bands in the absence or presence of monoazide **5** (Figure 2b). No difference in biotinylation of either HDAC3 or SMRT-DAD was observed with probes **3** and **4** in the presence of monoazide **5** despite the 10-fold molar excess of the latter and 990- and 150-fold difference in potency, respectively (Figure 1, 2b). This outcome was predicted based on the preliminary docking. Both probes **3** and **4** are short, and if they are chelated to Zn²⁺, their terminal phenyl ring containing the aryl and alkyl azides is positioned very close to the HDAC3 surface. In such binding poses, accessibility of the alkylazido moieties for the (3+2) cycloaddition is expected to be limited. To verify this, HDAC3-SMRT-DAD protein

complex was subjected to photocrosslinking with probes **2-4** and then denatured and reacted with the alkyne tag **7** in the absence or presence of monoazide **5** (Figure 2c). Probes **3** and **4** showed a dose-dependent biotinylation of HDAC3 but not SMRT-DAD. In the same experiment, probe **2** showed a dose dependent biotinylation of both HDAC3 and SMRT-DAD (Figure 2c; Supplementary Figure S8) similar to that observed in non-denaturing conditions, indicating that the outcome of the photocrosslinking and biotinylation steps observed in Figure 2b was not affected by the denaturing process. Thus, in the case of probes **3** and **4**, the accessibility of the alkylazido groups for (3+2) cycloaddition with the alkyne group of the biotin tag **9** is restricted whereas photocrosslinking reaction is not. Next, we determined whether probe **1** can crosslink with SMRT-DAD in the absence of HDAC3 and observed no increase in biotinylation at 2.5, 5, or 12.5 μ M concentration of probe **1** (Figure 2d). Next, we investigated if the observed photocrosslinking results can be influenced by the chemical structure of the probes and the competitors. We designed two novel amine based probes **7** and **8** bearing two surface binding groups (“arms”), where the shorter “arm” was represented by the photoreactive diazide moiety similar to that in probes **1-4**. We included probes **1** and **2** as controls to determine if the trend of crosslinking has been changed and we used TSA, a non-covalent competitor chemically different from monoazides **5** and **6**, to investigate whether the chemical structure and non-covalent nature of competition affected the outcome of the photolabeling. The experiment proceeded using a fixed concentration of the probes **7** and **8** (8.5 μ M) in the presence of a fixed concentration of TSA (42.5 μ M). Similarly to **1** and **2**, probes **7** and **8** photocrosslinked to both HDAC3 and SMRT-DAD and showed marginal biotinylation of both HDAC3 and SMRT-DAD in the presence of TSA (Figure 2b).

Finally, we investigated the ability of probe **2** to photocrosslink the cellular form of HDAC3-SMRT complex in the cell lysates of HT-29 cell lines. The choice of this particular cell line was driven by the multiple reports confirming the essentiality and overexpression of HDAC3 in colon carcinoma HT-29 cell line.^(36, 37) The concentration of probe **2** used in this experiment was set at the level sufficient to inhibit the deacetylation of HDACs in HT-29 cells and sustain a maximum acetylation of histones 3 and 4 in the range between 3 to 24 h (Supplementary Figure S7). The effect of U.V. irradiation on formation of possible reactive oxygen species in cell lysates or with recombinant proteins was limited by shortening the irradiation time (3 min) and irradiating the protein at lower temperature (4 °C).^(38, 39) Probe **2** at 25 μ M was able to photocrosslink HDAC3 (ca 49 kD) and two isoforms of SMRT (ca 170 and 230 kD) in a specific manner as the biotinylation signal of these bands disappear in the presence of an excess amount of the monoazide probe **5** (1 mM). We further confirmed these results by enriching the sample using streptavidin beads in the presence or absence of a different competitor (TSA) at a concentration of 500 μ M. The captured biotin adducts on the beads were identified as HDAC3 (ca 49 kD) and SMRT (ca 230 kD). These experiments have shown that similarly to the recombinant HDAC3-SMRT-DAD system, the full length SMRT is in proximity to the binding site of HDAC3 found in HT-29 cells.

Extensive *in silico* analysis of the protein surface and docking calculations were performed to assist in the interpretation of the experimental data. We generated 12 different homology models of HDAC3 that include residues 4-368 based on the X-ray data for HDAC8 using the program Modeller.⁽⁴⁰⁾ The homology models did not include 369-428 aa portion as it had no appropriate homologous sequences with 3D structures. For the SMRT-DAD an NMR structure, containing 28 conformers, each including SMRT residues 420-480, was available.⁽⁴¹⁾ The HDAC3 models were analyzed with cons-PSIP,⁽⁴²⁾ a program that combines a range of methodologies to predict the likelihood of each residue in a 3D protein structure for being involved in a protein-protein interface. The results (Figure 3; Supplementary Figure S1) suggest that the region proximal to the entrance to the channel leading to the HDAC3 catalytic site is most likely involved in protein-protein interactions.

For docking of SMRT-DAD to HDAC3 we employed two paradigms that can improve the docking accuracy. First, we used multiple protein structures to account for protein flexibility,⁽⁴³⁾ and second, instead of considering only the best scoring pose, we analyzed a multitude of high ranking poses by clustering, in an attempt to account qualitatively for entropic effects.⁽⁴⁴⁾ Using the program ZDOCK,⁽⁴⁵⁾ all 28 SMRT-DAD structures were docked to all 12 HDAC3 models, resulting in a total of 18 million complex models. In a hierarchical fashion these complex poses were re ranked using ZRANK,⁽⁴⁵⁾ and the 1000 top-ranking models were further refined using Firedock⁽⁴⁶⁾ allowing for limited protein flexibility. Finally the 100 best ranking poses were clustered using a k-means algorithm.⁽⁴⁷⁾ The resulting models were used for interpretation of the photolabeling studies without further optimization. Most high ranking solutions correspond to poses with the SMRT-DAD located close to the HDAC3 ligand-binding site (Supplementary Figure S1-S4). The centers of all clusters are shown in Figure S4a. The majority (77%) of high ranking poses and the biggest clusters correspond to a location of SMRT-DAD in the groove next to the HDAC3 active site entrance – *conformation 1* (Figure 3a). The location of SMRT in our model (Figure 3a) appears to be in agreement with the mutation studies conducted by Schwabe and co-authors.^(17, 41) The same projection of the HDAC3-SMRT-DAD complex including Ins(1,4,5,6)P₄ found in the X-ray model 4A69⁽¹⁷⁾ is shown in Figure 3b – *conformation 2*. A comparison of *conformations 1* and *2* shows that in *conformation 1* SMRT-DAD occupies roughly the position of Ins(1,4,5,6)P₄ in *conformation 2* (Figure 3).

Probes **1** and **2** were docked to multiple aligned HDAC3 structures using GOLD⁽⁴⁸⁾ and the coordinates of the reactive azide groups in the resulting poses were recorded. Next, removal of SMRT-DAD docking poses that either correspond to SMRT-DAD side chains extending into the binding site or located further than ca 6-7 Å, which is the approximate length of the photoreactive portion in probe **2**, resulted in a model of HDAC3-SMRT-DAD complex shown in Figure 3a (Supplementary pdb file). The maximum distance that can be reached by the diazide portion of probes **1** and **2** is rendered as red and green circles, respectively.

Photocrosslinking of the probes to HDAC3 was expected since the probes were bound to the HDAC3 active site at the time of photoactivation. Photocrosslinking with the SMRT-DAD (and full length SMRT), however, can occur only if the SMRT-DAD is positioned such that it can covalently react with the photoactivatable diazide portion of probes **1** or **2** while they are bound to HDAC3. Provided that the residence time of the hydroxamate-based HDAC inhibitors in the binding site of HDACs is substantially longer (ranging between seconds to minutes)^(49, 50) than the half-life of the typical products of the azide photolysis such as nitrenes (nanoseconds)⁽⁵¹⁾ and ketenimines (microseconds),^(52, 53) it is unlikely that the specific photolabeling of SMRT-DAD can occur after dissociation of the probes from the binding site. The fact that photoactivation of probes **3** and **4** does not result in photolabeling of SMRT-DAD further confirms that the photolabeling can occur only with the proteins that are in proximity to the probe bound to the active site. In our opinion, the above findings indicate that the only factors affecting the outcomes of the photolabeling of HDAC3 and SMRT-DAD are the distance between HDAC3 and SMRT-DAD and the length of the photoreactive probes-“nanorulers”.

The analysis of the docked poses of probe **2** (Figure 3a) shows that its diazide portion is limited to a semi-sphere with a radius of ca 6-7 Å, suggesting that SMRT-DAD is likely to be positioned no further than this distance. We validated this finding with probes **7** and **8** that had different surface binding groups but otherwise had the same length between the hydroxamic and the photoreactive moieties as in probe **2**. Despite the difference in the geometry and electrostatics between the amide and amino groups in probe **2** and probes **7** and **8**, respectively, and a change in the structure and the nature of the competitor from the covalent monoazides **5** and **6** to TSA, both new probes showed photolabeling and

competition by TSA at HDAC3 and SMRT-DAD identical to those of **1** and **2**. The photolabeling data obtained with probes **3** and **4**, on the other hand, had a different pattern, which may have two interpretations: 1) these probes may be too short to reach SMRT-DAD in the complex, and 2) they may also adopt poses where the aryl azide group is simply too far from SMRT-DAD but otherwise would be able to reach SMRT-DAD if the probe adopts a different binding pose. The latter interpretation would require SMRT-DAD to be positioned very close to the active site. Such proximity of SMRT-DAD would interfere with the binding of the vast majority of the HDAC3 inhibitors and, therefore, is unlikely to happen. To our surprise, in the X-ray structure, the distance between the terminal phenyl ring of probe **2** and the closest amino acid residue in SMRT-DAD is ca 10-13 Å (Figure 3b), which is too far to form a crosslinked adduct between probe **2** and SMRT-DAD. Altogether these findings indicate that in solution the SMRT-DAD is located closer to the binding site of HDAC3 compared to its position in the X-ray structure and may resemble the model shown in Figure 3a. Such close position of SMRT to the active site of HDAC3 may represent an opportunity to disrupt the HDAC3-SMRT complex by the surface binding groups of HDAC3 ligands. For instance, this may provide a rationale for disruption of HDAC4-NCOR complex by HDAC inhibitors FR235222 and FR276457.⁽⁵⁴⁾

Taking into account the photolabeling results and a possibility of SMRT-DAD occupying the position of Ins(1,4,5,6)P₄ suggested by the modeling studies, it was important to determine if Ins(1,4,5,6)P₄, which was reported to be detrimental for activity and stability of the HDAC3-SMRT-DAD complex,⁽¹⁷⁾ affects the enzymatic activity of HDAC3-SMRT-DAD and the photolabeling outcomes in our studies. The same authors reported that at concentrations of monovalent ions K⁺ and Na⁺ expected for a variety of physiological conditions,⁽⁵⁵⁾ the complex between HDAC3-SMRT-DAD was unstable and dissociated, requiring us to explore this aspect as well. If Ins(1,4,5,6)P₄ was solely responsible for activation of HDAC3-SMRT-DAD and assembly of HDAC3-SMRT-DAD into the complex, we should be able to clearly observe the differences in enzymatic activity and photolabeling. First, we assessed the enzymatic activity of the HDAC3-SMRT complex at three pre-incubation time points (5 min, 3 h, and 24 h) at room temperature. The complex retained activity for at least 3h (the pre-incubation period in which the photolabeling experiments were done), with a complete loss of activity after 24 h (Supplementary Figure S5a). Based on these observations, we excluded 24 h time point and only monitored the activity at 5 min and 3 h time points. In the next experiment, we monitored the activity of the complex at two time points (5 min and 3 h) in the absence or presence of Ins(1,4,5,6)P₄ at three different concentrations (0.1, 1, and 10 μM) and at a high 137 mM and low 25 mM concentrations of Na⁺ and 50 mM concentration of K⁺. The latter conditions are similar to those used by Schawbe et al.⁽¹⁷⁾ We also monitored the activity in the absence or presence of triton X at 0.1% and 0.3% (Supplementary Figure S5b). The initial conditions (Conditions 2; Supplementary Figure S5b) were the result of the optimization studies conducted by us and others to maximize the activity of the complex, signal to noise ratio, and stability for the experiments to determine IC₅₀ values of HDAC inhibitors. The conditions were also optimized to minimize possible protein aggregation that may influence the enzymatic activity of the complex as suggested by Bondos et al.⁽⁵⁶⁾ At both pre-incubation times, variation in Ins(1,4,5,6)P₄ and Na⁺ concentrations had little effect on the absolute enzymatic activity of HDAC3-SMRT-DAD, 25000 vs 29000 AFU, respectively. A ca 8-10% drop in activity was observed at 50 mM of K⁺ and 0.1% of triton X and a much more pronounced drop - at 0.3% of triton X after 5 min pre incubation. The effect was much less pronounced at 3 h pre-incubation compared to 5 min. These experiments demonstrate that Ins(1,4,5,6)P₄ has a rather limited effect on the activity of the HDAC3-SMRT-DAD complex even at very low 25 mM concentration of NaCl. These observations indicate that neither Ins(1,4,5,6)P₄ nor the varied concentrations of monovalent ions tested affect the association of the HDAC3-SMRT-DAD complex as otherwise its enzymatic activity would

be negligible.^(13, 41, 57) The lower enzymatic activity in the presence of the 3-fold higher concentration of triton X is not surprising taking into account its detergent properties and known binding to hydrophobic channels in proteins.⁽⁵⁸⁾ According to our preliminary docking, triton X-100 fits the binding site and can adopt the binding pose similar to those of the known HDAC inhibitors. A very high 2000-fold excess of acetate ion (in the form of CH₃COOK), which is the product of the deacetylation of the fluorogenic substrate Boc-Lys(Ac)-AMC and is also known to bind to the active site of HDAC3, may explain the lower enzymatic activity of the HDAC3-SMRT-DAD complex observed in the presence of 50 mM of CH₃COOK (Conditions 5 and 6, Supplementary Figure S5). The latter observation suggests that high concentrations of the acetate salts in buffers with HDAC3-SMRT should be avoided.

Next, we characterized the effect of Ins(1,4,5,6)P₄ and monovalent metal ions in a series of photolabeling experiments with probes **2** and **5**. Probe **2** (1.7 and 8.5 μM) in the presence or absence of monoazide competitor **5** (42.5 μM) was photocrosslinked with HDAC3-SMRT-DAD complex at a high and low concentration of Na⁺ and K⁺ ions and in the presence or absence of 1.7, 8.5, or 42.5 μM of Ins(1,4,5,6)P₄. These experiments and their conditions are provided in Figure 4 and Supplementary Figure S6. The complex was pre-incubated for 1.5 h in the buffer with or without Ins(1,4,5,6)P₄ before addition of the probes to eliminate any effect the probes might have on the complex formation in solution. Probe **2** was capable of crosslinking both HDAC3 and SMRT-DAD regardless of the concentration of the monovalent ions and it was competed out by probe **5** similarly to that shown in Figure 2b. In the presence of Ins(1,4,5,6)P₄, probe **2** was still capable of photocrosslinking both HDAC3 and SMRT, however Ins(1,4,5,6)P₄ appears to behave as a competitor of photolabeling. Unlike the monoazide competitor **5** investigated in this paper as well as other monoazide competitors and HDAC inhibitors,⁽²²⁾ Ins(1,4,5,6)P₄ showed a unique effect on photolabeling of HDAC3-SMRT-DAD complex not observed with other competitors. Specifically, an increasing concentration of Ins(1,4,5,6)P₄ did not affect the biotinylation of HDAC3 (Figure 4c) whereas the biotinylation of SMRT-DAD was decreased in a dose dependent and a statistically significant fashion (Figure 4c).

To investigate the effect different experimental conditions may have on inhibition of the HDAC3-SMRT-DAD enzymatic activity by probe **2**, we determined its IC₅₀s in the presence or absence of Ins(1,4,5,6)P₄, potassium acetate, and triton X (Supplementary Tables S1 and S2). We found that in all cases the effect of Ins(1,4,5,6)P₄ on IC₅₀ value of probe **2** was comparable or even smaller than that of the other components of the buffers, such as monovalent metal ions, acetate ions, and triton X. However, we observed an interesting trend - regardless of the nature of other components of the buffers, IC₅₀ values of probe **2** with Ins(1,4,5,6)P₄ were 18–26% better than those without Ins(1,4,5,6)P₄ in otherwise identical conditions. Any other deviation from the “in-house” conditions resulted in at least 1.2-fold (at 5 min) higher IC₅₀ values, a trend opposite to that observed with Ins(1,4,5,6)P₄. Considering that Ins(1,4,5,6)P₄ does not inhibit the enzymatic activity of HDAC3-SMRT-DAD by itself (Supplementary Figure S5), it appears that the presence of Ins(1,4,5,6)P₄ has a small synergistic effect on inhibition of the complex by probe **2**, which may be expected if Ins(1,4,5,6)P₄ causes the distance between the binding site of HDAC3 and SMRT-DAD to increase.

Puzzled by these findings, we decided to investigate the effect Ins(1,4,5,6)P₄ may have on the photolabeling with probe **1**, the longest in this series. Our docking studies have shown that unlike probe **2**, probe **1** can reach SMRT-DAD in both our model shown in Figure 3a and in the X-ray model shown in Figure 3b. Since both conformations can be reached by probe **1**, we anticipated that the decrease in biotinylation of SMRT-DAD by probe **1** in response to increasing concentration of Ins(1,4,5,6)P₄ will be not as pronounced as in the

case of probe **2** even if there is a change in the conformation of the HDAC3-SMRT-DAD complex. Consistently with this model, we found that Ins(1,4,5,6)P₄ had no statistically significant effect on photolabeling of either HDAC3 or SMRT-DAD with probe **1** at all the concentrations tested in the presence or absence of the competitor, monoazide **5** (Figure 4).

To provide further corroborating evidence that the position of SMRT-DAD in the complex with HDAC3 in solution is in agreement with the photocrosslinking results, we performed a series of NMR saturation transfer difference (STD) experiments with probe **7** and/or Ins(1,4,5,6)P₄ in a buffer solution with HDAC3-SMRT-DAD. This method allows investigation of binding epitopes of small ligands that are in contact with high molecular weight proteins.^(59, 60) Probe **7** was chosen because of its intermediate affinity for the HDAC3-SMRT-DAD complex that allows favorable detection by STD. The results of the experiment are shown in Figure 4. When probe **7** (100 μM) was added to the HDAC3-SMRT-DAD complex (1 μM) we observed an STD response from its aromatic and alkyl portions, indicating that they participate in binding to the complex (Figure 4a). Addition of 25 μM Ins(1,4,5,6)P₄ prevented detection of the aromatic groups in the STD spectra. Only the STD signals most likely corresponding to the methylenes adjacent to the amine nitrogen atom were observed (Figure 5b). More precise assignment was not possible due to chemical shift changes. We also detected the STD response when 25 μM of Ins(1,4,5,6)P₄ was incubated with the HDAC3-SMRT-DAD complex without probe **7** (Figure 5c). Control experiments with HDAC3-SMRT-DAD complex alone, and probe **7** alone with and without Ins(1,4,5,6)P₄ showed no STD signals (data not shown). There are several important conclusions that can be derived from these experiments. First, they confirm the previous finding by Schwabe et al that Ins(1,4,5,6)P₄ binds to the HDAC3-SMRT-DAD complex. The fact that the STD response for Ins(1,4,5,6)P₄ was observed only after its addition to the HDAC3-SMRT-DAD complex indicates that Ins(1,4,5,6)P₄ was not present in the complex during purification in the amounts sufficient to generate an STD response and its binding is relatively weak but perhaps comparable to that of probe **7**. Second, addition of Ins(1,4,5,6)P₄ leads to conformational changes in the complex between the HDAC3-SMRT-DAD and probe **7**. Third, the nature of the STD signals for probe **7** without and with Ins(1,4,5,6)P₄ is consistent with the conformation of the HDAC3-SMRT-DAD complex in our model (Figure 3a) and the X-ray model (Figure 3b), respectively. In the X-ray model the aromatic ring of probe **7** would not be in direct contact with SMRT-DAD and is not expected to give the STD response. Clearly, both the STD NMR and the photocrosslinking data are in agreement.

The data presented raise an important question, can the HDAC3-SMRT-DAD complex in solution adopt both the conformation proposed in our model (*conformation 1*, Figure 3a) and the one observed in the X-ray model (*conformation 2*, Figure 3b)?⁽¹⁷⁾ It certainly appears so based on the experimental evidence provided above. The next important question is whether Ins(1,4,5,6)P₄ is as important for the complex with the full-length HDAC3 as it was reported for the truncated one? The outcomes of our enzymatic, photolabeling, and NMR studies clearly indicate that Ins(1,4,5,6)P₄ may not play the same role. Although according to the STD NMR experiments it binds HDAC3-SMRT-DAD complex, it is not present in the purified HDAC3-SMRT-DAD complex. Moreover, despite a considerable 43- to 4300-fold excess in the concentration of Ins(1,4,5,6)P₄ to that of the HDAC3-SMRT-DAD complex in our experiments, Ins(1,4,5,6)P₄ has displayed negligible effect on the enzymatic activity of the complex and is not capable of dissociating HDAC3-SMRT-DAD. Instead, the increase in the concentration of Ins(1,4,5,6)P₄ appears to result in switching between *conformation 1* where the photoreactive probes can crosslink with SMRT-DAD and *conformation 2* where SMRT-DAD is too far for the photocrosslinking to occur. In *conformation 1* SMRT-DAD abstracts the positively charged site containing His17, Lys25, Arg265, and Arg301 and prevents Ins(1,4,5,6)P₄ from binding to HDAC3. As the concentration of Ins(1,4,5,6)P₄

increases, it starts to compete with SMRT-DAD for the positively charged site on HDAC3. The equilibrium between the two conformations shifts toward *conformation 2* where the distance between the binding site of HDAC3 and SMRT-DAD is longer, which explains why in the case of probe **2** biotinylation of SMRT-DAD decreases whereas biotinylation of HDAC3 does not and in the case of longer probe **1** biotinylation of both SMRT-DAD and HDAC3 remains constant upon addition of Ins(1,4,5,6)P₄. The switch between *conformations 1* and *2* is also consistent with the small synergistic effect of Ins(1,4,5,6)P₄ on the inhibition of HDAC3-SMRTR-DAD complex by probe **2**. The STD NMR experiments strongly support both the phenomenon of the conformational switch and the differences in the distances in the conformations occurring in the absence and presence of Ins(1,4,5,6)P₄.

On the basis of this data we propose that strongly negatively charged molecules, such as Ins(1,4,5,6)P₄, or DNA, or even the C-terminal portion (truncated in the X-ray structure amino acids 379-428) of HDAC3, which is rich in aspartic and glutamic acids, may play a regulatory role in switching between the two (or more) conformations of HDAC3-SMRT complex as shown in Figure 6. It is tempting to speculate that changes in the HDAC3 and SMRT relative orientation, geometry of the binding site, and charge distribution associated with *conformations 1* and *2* may be necessary to appropriately position HDAC3 for the unidirectional deacetylation of K5Ac→K8Ac→K12Ac →K16Ac in histone H4,^(12, 61) a so-called feed-forward model of deacetylation (Figure 6, step 1),^(12, 14) to provide substrate specificity for histone and non histone targets, to stabilize the co-repressor complex, and to block access to HATs.⁽¹²⁾ Considering proximity of K16 in H4 to DNA in nucleosomes (for instance in PDB: 1AOI),⁽⁶²⁾ strong electrostatic attraction between the positively charged HDAC3 residues His17, Lys25, Arg265, and Arg301, the binding site for Ins(1,4,5,6)P₄ in the X-ray model, and DNA would be expected after HDAC3-SMRT deacetylates K16. Such binding may then cause HDAC3-SMRT-DAD to adopt *conformation 2* (Figure 6, step 2) much like it happens in the presence of Ins(1,4,5,6)P₄. In fact, re organization of the SMRT complex is required to release the interaction between HID, a histone interaction domain located in the second SANT domain of SMRT,^(14, 63) and the deacetylated H4 histone tail to allow it to bind to DNA. Upon release, the mostly positively charged SANT2 domain (PDB: 2LTP)⁽⁶⁴⁾ would then be expected to engage in the interaction with DNA (Figure 6, step 2). Structural similarity of the SANT domains with Myb⁽⁴¹⁾ and SLIDE⁽⁶⁵⁾ DNA binding domains further supports this scenario. The switch between *conformations 1* and *2* upon binding of HDAC3 and/or SANT2 to DNA may, therefore, serve as a termination signal for the histone deacetylation machinery as a result of re-orientation of the catalytic site of HDAC3 away from the histone tail (Figure 6, step 2). In concert with the other components of the histone code,⁽⁶⁶⁾ such conformational switch may not only be responsible for maintaining the proper order of deacetylation but may also provide a “failsafe” mechanism if the deacetylation proceeds in an incorrect order. Despite the difference in the protein components of the deacetylase complexes involving HDAC1/2 and HDAC3, many of the HDAC3 and SMRT structural features discussed above are also found in the HDAC1 and HDAC2 deacetylase complexes. For instance, similarly to SMRT, CoREST contains two SANT domains,⁽⁶⁷⁾ and both HDAC1 and HDAC2 contain the same positively charged pocket formed by His17, Lys25, Arg265, and Arg301 that is found in HDAC3. Such conservation of the features suggests a possibility that the observations presented in this manuscript may have implications beyond the HDAC3-SMRT complex.

In summary, six novel photoreactive HDAC probes - “nanorulers” - were designed and applied to measure the distance between the binding site of HDAC3 and SMRT-DAD in solution using a variety of enzymatic, photocrosslinking, and STD NMR experiments. Unlike previous studies, the experiments were conducted with the full-length HDAC3 in the complex with both the recombinant SMRT-DAD as well the full-length SMRT from cell

lysates. Our study finds that under physiologically relevant conditions in solution-SMRT-DAD is positioned ca 10–13 Å closer to the binding site of HDAC3 – *conformation 1* – than in the X-ray model – *conformation 2*. Multiple independent lines of evidence with the photoreactive probes presented in the manuscript suggest that Ins(1,4,5,6)P₄ can cause a switch between *conformations 1* and 2 without affecting the enzymatic activity of the HDAC3 and SMRT-DAD complex. To the best of our knowledge this is the first example where the photoreactive probes were used to detect conformational changes occurring in transcription complexes in response to chemical stimuli. We propose that the observed conformational switch plays an important role in “interpreting” the histone code. Further studies including design of “nanoprotractors” and development of novel approaches to modulate the epigenetic machinery based on our findings are underway.

Supplementary Material

Refer to Web version on PubMed Central for supplementary material.

Acknowledgments

This study was funded by the National Cancer Institute/NIH Grants R01CA131970 to P.A.P and R01CA135331 to V.G. Molecular modeling studies were in part performed with the UCSF Chimera package from the Resource for Biocomputing, Visualization, and Informatics at the University of California, San Francisco (supported by NIH P41 RR-01081) and Open Eye Scientific Software, Santa Fe, NM. We thank K. Bruzik (UIC) for providing us with D-myo inositol (1,4,5,6) tetrakisphosphate sodium salt. We also thank J. Frasor (UIC) for careful reading of the manuscript and for providing many helpful comments.

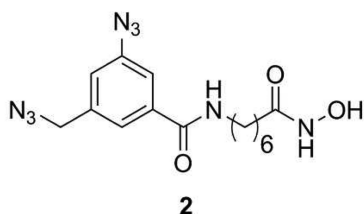
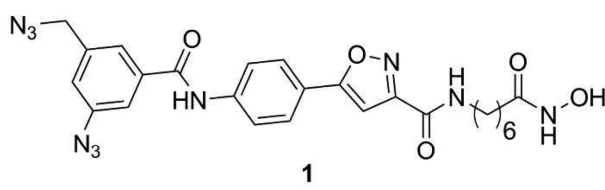
REFERENCES

1. Wolffe AP, Guschin D. Review: chromatin structural features and targets that regulate transcription. *J. Struct. Biol.* 2000; 129:102–122. [PubMed: 10806063]
2. Acharya MR, Sparreboom A, Venitz J, Figg WD. Rational development of histone deacetylase inhibitors as anticancer agents: a review. *Mol. Pharmacol.* 2005; 68:917–932. [PubMed: 15955865]
3. Godman CA, Joshi R, Tierney BR, Greenspan E, Rasmussen TP, Wang HW, Shin DG, Rosenberg DW, Giardina C. HDAC3 impacts multiple oncogenic pathways in colon cancer cells with effects on Wnt and vitamin D signaling. *Cancer Biol. Ther.* 2008; 7:1570–1580. [PubMed: 18769117]
4. McQuown SC, Barrett RM, Matheos DP, Post RJ, Rogge GA, Alenghat T, Mullican SE, Jones S, Rusche JR, Lazar MA, Wood MA. HDAC3 is a critical negative regulator of long-term memory formation. *J. Neurosci.* 2011; 31:764–774. [PubMed: 21228185]
5. Zhang F, Shi Y, Wang L, Sriram S. Role of HDAC3 on p53 expression and apoptosis in T cells of patients with multiple sclerosis. *PLoS One.* 2011; 6:e16795. [PubMed: 21346816]
6. Rai M, Soragni E, Chou CJ, Barnes G, Jones S, Rusche JR, Gottesfeld JM, Pandolfo M. Two New Pimelic Diphenylamide HDAC Inhibitors Induce Sustained Frataxin Upregulation in Cells from Friedreich's Ataxia Patients and in a Mouse Model. *PLoS One.* 2010; 5
7. Fischer A, Sananbenesi F, Mungenast A, Tsai LH. Targeting the correct HDAC(s) to treat cognitive disorders. *Trends Pharmacol. Sci.* 2010; 31:605–617. [PubMed: 20980063]
8. Dietz KC, Casaccia P. HDAC inhibitors and neurodegeneration: at the edge between protection and damage. *Pharmacol. Res.* 2010; 62:11–17. [PubMed: 20123018]
9. McKinsey TA. Isoform-selective HDAC inhibitors: closing in on translational medicine for the heart. *J. Mol. Cell. Cardiol.* 2011; 51:491–496. [PubMed: 21108947]
10. Hayakawa T, Nakayama J. Physiological roles of class I HDAC complex and histone demethylase. *J. Biomed. Biotechnol.* 2011; 2011:129383. [PubMed: 21049000]
11. Li JW, Wang J, Wang JX, Nawaz Z, Liu JM, Qin J, Wong JM. Both corepressor proteins SMRT and N-CoR exist in large protein complexes containing HDAC3. *EMBO J.* 2000; 19:4342–4350. [PubMed: 10944117]

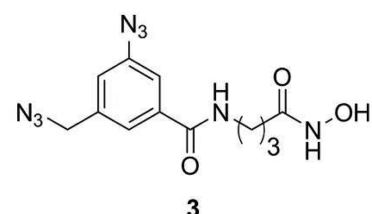
12. Hartman HB, Yu J, Alenghat T, Ishizuka T, Lazar MA. The histone binding code of nuclear receptor co-repressors matches the substrate specificity of histone deacetylase 3. *EMBO Rep.* 2005; 6:445–451. [PubMed: 15832170]
13. Guenther MG, Barak O, Lazar MA. The SMRT and N-CoR corepressors are activating cofactors for histone deacetylase 3. *Mol. Cell. Biol.* 2001; 21:6091–6101. [PubMed: 11509652]
14. Yu J, Li Y, Ishizuka T, Guenther MG, Lazar MA. A SANT motif in the SMRT corepressor interprets the histone code and promotes histone deacetylation. *EMBO J.* 2003; 22:3403–3410. [PubMed: 12840002]
15. Lazar MA. Nuclear receptor corepressors. *Nucl. Recept. Signaling.* 2003; 1:e001.
16. You SH, Lim HW, Sun Z, Broache M, Won KJ, Lazar MA. Nuclear receptor co-repressors are required for the histone-deacetylase activity of HDAC3 in vivo. *Nat. Struct. Mol. Biol.* 2013; 20:182–187. [PubMed: 23292142]
17. Watson PJ, Fairall L, Santos GM, Schwabe JW. Structure of HDAC3 bound to co-repressor and inositol tetraphosphate. *Nature.* 2012; 481:335–340. [PubMed: 22230954]
18. Oberoi J, Fairall L, Watson PJ, Yang JC, Czimmeier Z, Kampmann T, Goult BT, Greenwood JA, Gooch JT, Kallenberger BC, Nagy L, Neuhaus D, Schwabe JW. Structural basis for the assembly of the SMRT/NCoR core transcriptional repression machinery. *Nat. Struct. Mol. Biol.* 2011; 18:177–184. [PubMed: 21240272]
19. Codina A, Love JD, Li Y, Lazar MA, Neuhaus D, Schwabe JW. Structural insights into the interaction and activation of histone deacetylase 3 by nuclear receptor corepressors. *Proc. Natl. Acad. Sci. U. S. A.* 2005; 102:6009–6014. [PubMed: 15837933]
20. Vaidya AS, Neelarapu R, Bai H, Madriaga A, Mendonca E, Brunsteiner M, van Breemen R, Blond SY, Petukhov PA. Novel Histone Deacetylase 8 Ligands without a Bidentate Zinc Chelating Group: Exploring an Upside-down Binding Pose. *Bioorg. Med. Chem. Lett.* 2012; 22:6621–6627. [PubMed: 23010266]
21. Vaidya AS, Karumudi B, Mendonca E, Madriaga A, Abdelkarim H, van Breemen RB, Petukhov PA. Design, synthesis, modeling, biological evaluation and photoaffinity labeling studies of novel series of photoreactive benzamide probes for histone deacetylase 2. *Bioorg. Med. Chem. Lett.* 2012; 22:5025–5030. [PubMed: 22771007]
22. He B, Velaparthi S, Pieffet G, Pennington C, Mahesh A, Holzle DL, Brunsteiner M, van Breemen R, Blond SY, Petukhov PA. Binding ensemble profiling with photoaffinity labeling (BEPFL) approach: mapping the binding poses of HDAC8 inhibitors. *J. Med. Chem.* 2009; 52:7003–7013. [PubMed: 19886628]
23. Yang WM, Tsai SC, Wen YD, Fejer G, Seto E. Functional domains of histone deacetylase-3. *J. Biol. Chem.* 2002; 277:9447–9454. [PubMed: 11779848]
24. Phizicky EM, Fields S. Protein-protein interactions: methods for detection and analysis. *Microbiol. Rev.* 1995; 59:94–123. [PubMed: 7708014]
25. Guan H, Kiss-Toth E. Advanced technologies for studies on protein interactomes. *Adv. Biochem. Eng./Biotechnol.* 2008; 110:1–24.
26. Mandell JG, Baerga-Ortiz A, Croy CH, Falick AM, Komives EA. Application of amide proton exchange mass spectrometry for the study of protein-protein interactions. *Curr. Protoc. Protein. Sci.* 2005 Chapter 20, Unit20 29.
27. Busenlehner LS, Armstrong RN. Insights into enzyme structure and dynamics elucidated by amide H/D exchange mass spectrometry. *Arch. Biochem. Biophys.* 2005; 433:34–46. [PubMed: 15581564]
28. Hoofnagle AN, Resing KA, Ahn NG. Protein analysis by hydrogen exchange mass spectrometry. *Annu. Rev. Biophys. Biomol. Struct.* 2003; 32:1–25. [PubMed: 12598366]
29. Maier CS, Deinzer ML. Protein conformations, interactions, and H/D exchange. *Methods Enzymol.* 2005; 402:312–360. [PubMed: 16401514]
30. Garcia RA, Pantazatos D, Villarreal FJ. Hydrogen/deuterium exchange mass spectrometry for investigating protein-ligand interactions. *Assay Drug Dev. Technol.* 2004; 2:81–91. [PubMed: 15090213]
31. Hosoya T, Hiramatsu T, Ikemoto T, Nakanishi M, Aoyama H, Hosoya A, Iwata T, Maruyama K, Endo M, Suzuki M. Novel bifunctional probe for radioisotope-free photoaffinity labeling: compact

- structure comprised of photospecific ligand ligation and detectable tag anchoring units. *Org. Biomol. Chem.* 2004; 2:637–641. [PubMed: 14985799]
- 32. Neelarapu R, Holzle DL, Velaparthi S, Bai H, Brunsteiner M, Blond SY, Petukhov PA. Design, synthesis, docking, and biological evaluation of novel diazide-containing isoxazole- and pyrazole based histone deacetylase probes. *J. Med. Chem.* 2011; 54:4350–4364. [PubMed: 21548582]
 - 33. Brunsteiner M, Petukhov PA. Insights from comprehensive multiple receptor docking to HDAC8. *J. Mol. Model.* 2012; 18:3927–3939. [PubMed: 22431224]
 - 34. Liu S, Zhou B, Yang H, He Y, Jiang ZX, Kumar S, Wu L, Zhang ZY. Aryl vinyl sulfonates and sulfones as active site-directed and mechanism-based probes for protein tyrosine phosphatases. *J. Am. Chem. Soc.* 2008; 130:8251–8260. [PubMed: 18528979]
 - 35. Speers AE, Cravatt BF. Profiling enzyme activities in vivo using click chemistry methods. *Chem. Biol.* 2004; 11:535–546. [PubMed: 15123248]
 - 36. Spurling CC, Godman CA, Noonan EJ, Rasmussen TP, Rosenberg DW, Giardina C. HDAC3 overexpression and colon cancer cell proliferation and differentiation. *Mol. Carcinog.* 2008; 47:137–147. [PubMed: 17849419]
 - 37. Wilson AJ, Byun DS, Popova N, Murray LB, L'Italien K, Sowa Y, Arango D, Velcich A, Augenlicht LH, Mariadason JM. Histone deacetylase 3 (HDAC3) and other class I HDACs regulate colon cell maturation and p21 expression and are deregulated in human colon cancer. *J. Biol. Chem.* 2006; 281:13548–13558. [PubMed: 16533812]
 - 38. Verweij H, Dubbelman TM, Van Steveninck J. Photodynamic protein cross linking. *Biochim. Biophys. Acta.* 1981; 647:87–94. [PubMed: 7295723]
 - 39. Pattison DI, Rahmanto AS, Davies MJ. Photo oxidation of proteins. *Photochem. Photobiol. Sci.* 2012; 11:38–53. [PubMed: 21858349]
 - 40. Sali A, Blundell TL. Comparative protein modelling by satisfaction of spatial restraints. *J. Mol. Biol.* 1993; 234:779–815. [PubMed: 8254673]
 - 41. Codina A, Love JD, Li Y, Lazar MA, Neuhaus D, Schwabe JWR. Structural insights into the interaction and activation of histone deacetylase 3 by nuclear receptor corepressors. *Proc. Natl. Acad. Sci. U. S. A.* 2005; 102:6009–6014. [PubMed: 15837933]
 - 42. Qin S, Zhou HX. meta-PPISP: a meta web server for protein-protein interaction site prediction. *Bioinformatics.* 2007; 23:3386–3387. [PubMed: 17895276]
 - 43. Novoa EM, de Pouplana LR, Barril X, Orozco M. Ensemble Docking from Homology Models. *J. Chem. Theory Comput.* 2010; 6:2547–2557.
 - 44. Lee J, Seok C. A statistical rescoring scheme for protein-ligand docking: Consideration of entropic effect. *Proteins.* 2008; 70:1074–1083. [PubMed: 18076034]
 - 45. Pierce B, Weng Z. ZRANK: reranking protein docking predictions with an optimized energy function. *Proteins.* 2007; 67:1078–1086. [PubMed: 17373710]
 - 46. Andrusier N, Nussinov R, Wolfson HJ. FireDock: fast interaction refinement in molecular docking. *Proteins.* 2007; 69:139–159. [PubMed: 17598144]
 - 47. Kanungo T, Mount DM, Netanyahu NS, Piatko CD, Silverman R, Wu AY. An efficient k means clustering algorithm: Analysis and implementation. *IEEE Transactions on Pattern Analysis and Machine Intelligence.* 2002; 24:881–892.
 - 48. Verdonk ML, Cole JC, Hartshorn MJ, Murray CW, Taylor RD. Improved protein-ligand docking using GOLD. *Proteins.* 2003; 52:609–623. [PubMed: 12910460]
 - 49. Singh RK, Mandal T, Balasubramanian N, Cook G, Srivastava DK. Coumarin-suberoylanilide hydroxamic acid as a fluorescent probe for determining binding affinities and off-rates of histone deacetylase inhibitors. *Anal. Biochem.* 2011; 408:309–315. [PubMed: 20816742]
 - 50. Lauffer BE, Mintzer R, Fong R, Mukund S, Tam C, Zilberleyb I, Flicke B, Ritscher A, Fedorowicz G, Vallero R, Ortwine DF, Gunzner J, Modrusan Z, Neumann L, Koth CM, Lupardus PJ, Kaminker JS, Heise CE, Steiner P. Histone deacetylase (HDAC) inhibitor kinetic rate constants correlate with cellular histone acetylation but not transcription and cell viability. *J. Biol. Chem.* 2013
 - 51. Gritsan NP, Yuzawa T, Platz MS. Direct observation of singlet phenylnitrene and measurement of its rate of rearrangement. *J. Am. Chem. Soc.* 1997; 119:5059–5060.

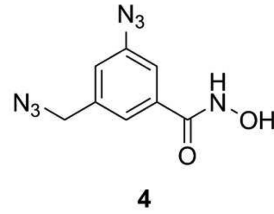
52. Schrock AK, Schuster GB. Photochemistry of Phenyl Azide - Chemical-Properties of the Transient Intermediates. *J. Am. Chem. Soc.* 1984; 106:5228–5234.
53. Li YZ, Kirby JP, George MW, Poliakoff M, Schuster GB. 1,2-Dihydroazepines from the Photolysis of Substituted Aryl - Azides Analysis of Their Chemical and Physical-Properties by Time-Resolved Spectroscopic Methods. *J. Am. Chem. Soc.* 1988; 110:8092–8098.
54. Matsuoka H, Fujimura T, Hayashi M, Matsuda K, Ishii Y, Aramori I, Mutoh S. Disruption of HDAC4/N-CoR complex by histone deacetylase inhibitors leads to inhibition of IL-2 gene expression. *Biochem. Pharmacol.* 2007; 74:465–476. [PubMed: 17559812]
55. Takagi K, Okabe Y, Yoshimura K, Ichikawa Y. Changes in intracellular K⁺ and Na⁺ ion concentrations during cell growth and differentiation. *Cell Struct Funct.* 1986; 11:235–243. [PubMed: 3464361]
56. Bondos SE, Bicknell A. Detection and prevention of protein aggregation before, during, and after purification. *Anal. Biochem.* 2003; 316:223–231. [PubMed: 12711344]
57. Wen YD, Perissi V, Staszewski LM, Yang WM, Krones A, Glass CK, Rosenfeld MG, Seto E. The histone deacetylase-3 complex contains nuclear receptor corepressors. *Proc. Natl. Acad. Sci. U. S. A.* 2000; 97:7202–7207. [PubMed: 10860984]
58. Gao W, Starkov VG, He ZX, Wang QH, Tsetlin VI, Utkin YN, Lin ZJ, Bi RC. Functions, structures and Triton X-100 effect for the catalytic subunits of heterodimeric phospholipases A2 from Vipera nikolskii venom. *Toxicon.* 2009; 54:709–716. [PubMed: 19500614]
59. Mayer M, Meyer B. Group epitope mapping by saturation transfer difference NMR to identify segments of a ligand in direct contact with a protein receptor. *J. Am. Chem. Soc.* 2001; 123:6108–6117. [PubMed: 11414845]
60. Viegas A, Manso J, Corvo MC, Marques MM, Cabrita EJ. Binding of ibuprofen, ketorolac, and diclofenac to COX-1 and COX-2 studied by saturation transfer difference NMR. *J. Med. Chem.* 2011; 54:8555–8562. [PubMed: 22091869]
61. Zhang K, Williams KE, Huang L, Yau P, Siino JS, Bradbury EM, Jones PR, Minch MJ, Burlingame AL. Histone acetylation and deacetylation: identification of acetylation and methylation sites of HeLa histone H4 by mass spectrometry. *Mol. Cell. Proteomics.* 2002; 1:500–508. [PubMed: 12239278]
62. Luger K, Mader AW, Richmond RK, Sargent DF, Richmond TJ. Crystal structure of the nucleosome core particle at 2.8 Å resolution. *Nature.* 1997; 389:251–260. [PubMed: 9305837]
63. Boyer LA, Latek RR, Peterson CL. The SANT domain: a unique histone tail binding module? *Nat. Rev. Mol. Cell Biol.* 2004; 5:158–163. [PubMed: 15040448]
64. Montecchio M, Lemak A, Yee A, Xu C, Garcia M, Houlston S, Bellanda M, Min J, Montelione GT, Arrowsmith C. PDB: 2LTP. To be published.
65. Hota SK, Bhardwaj SK, Deindl S, Lin YC, Zhuang X, Bartholomew B. Nucleosome mobilization by ISW2 requires the concerted action of the ATPase and SLIDE domains. *Nat. Struct. Mol. Biol.* 2013
66. Strahl BD, Allis CD. The language of covalent histone modifications. *Nature.* 2000; 403:41–45. [PubMed: 10638745]
67. Andres ME, Burger C, Peral-Rubio MJ, Battaglioli E, Anderson ME, Grimes J, Dallman J, Ballas N, Mandel G. CoREST: a functional corepressor required for regulation of neural-specific gene expression. *Proc. Natl. Acad. Sci. U. S. A.* 1999; 96:9873–9878. [PubMed: 10449787]



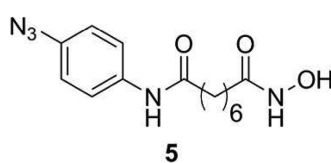
HDAC3 IC₅₀ ± SD = 32.1 ± 5.1 nM



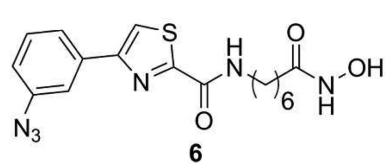
HDAC3 IC₅₀ ± SD = 19500 ± 820 nM



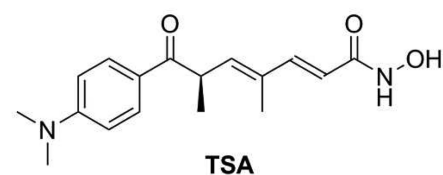
HDAC3 IC₅₀ ± SD = 2950 ± 190 nM



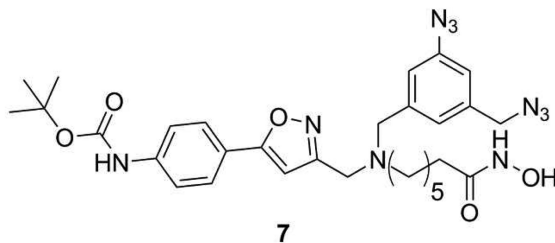
HDAC3 IC₅₀ ± SD = 19.7 ± 2.0 nM



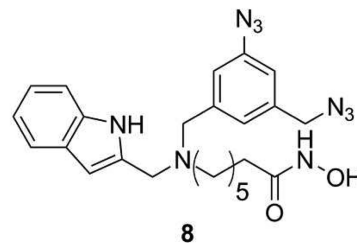
HDAC3 IC₅₀ ± SD = 11.6 ± 0.46 nM



HDAC3 IC₅₀ ± SD = 3.2 ± 1.0 nM



HDAC3 IC₅₀ ± SD = 593 ± 20.3 nM



HDAC3 IC₅₀ ± SD = 894 ± 36.7 nM

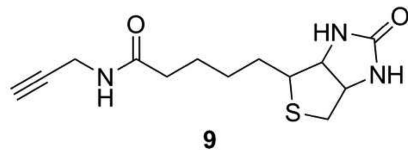
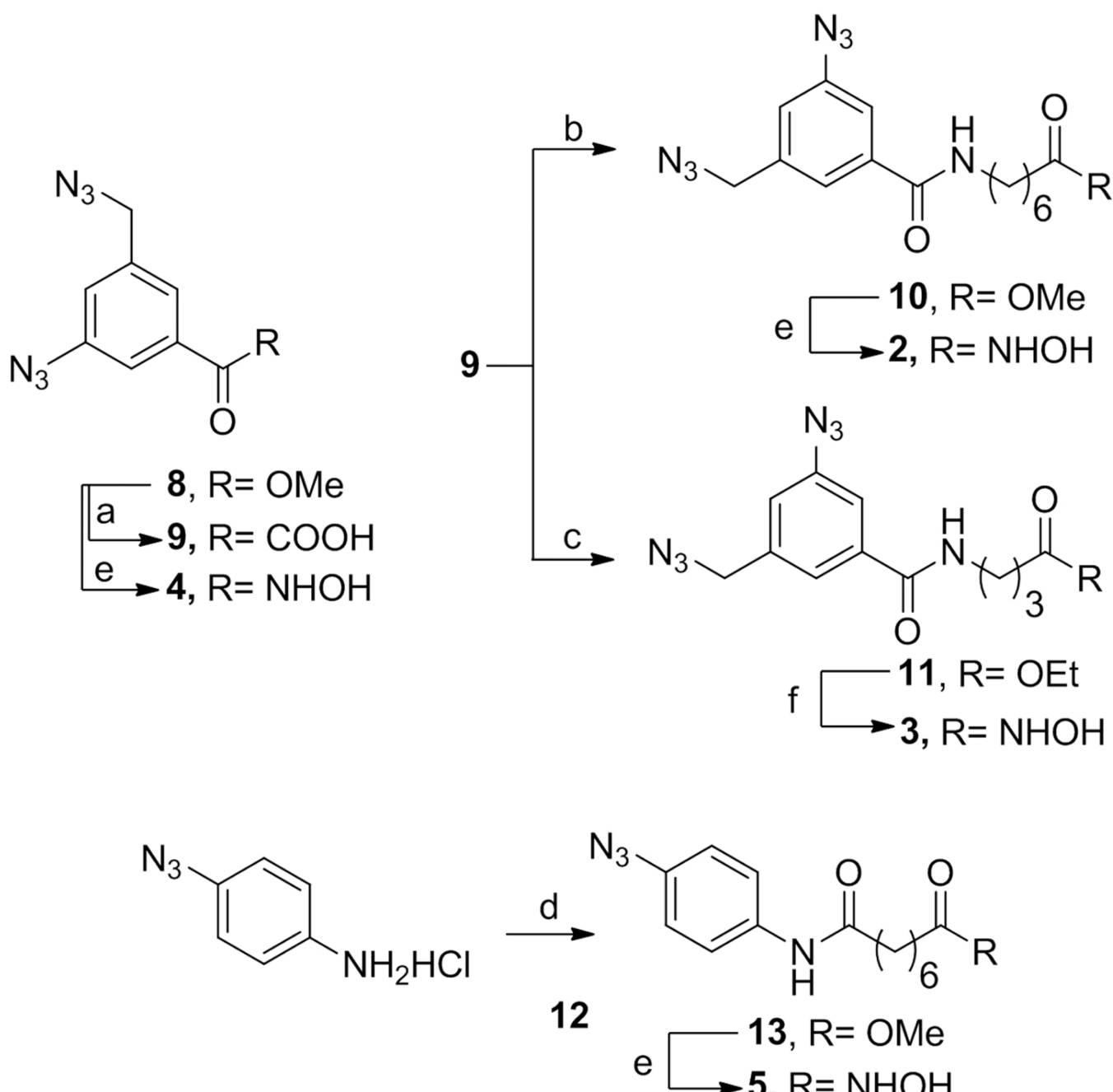
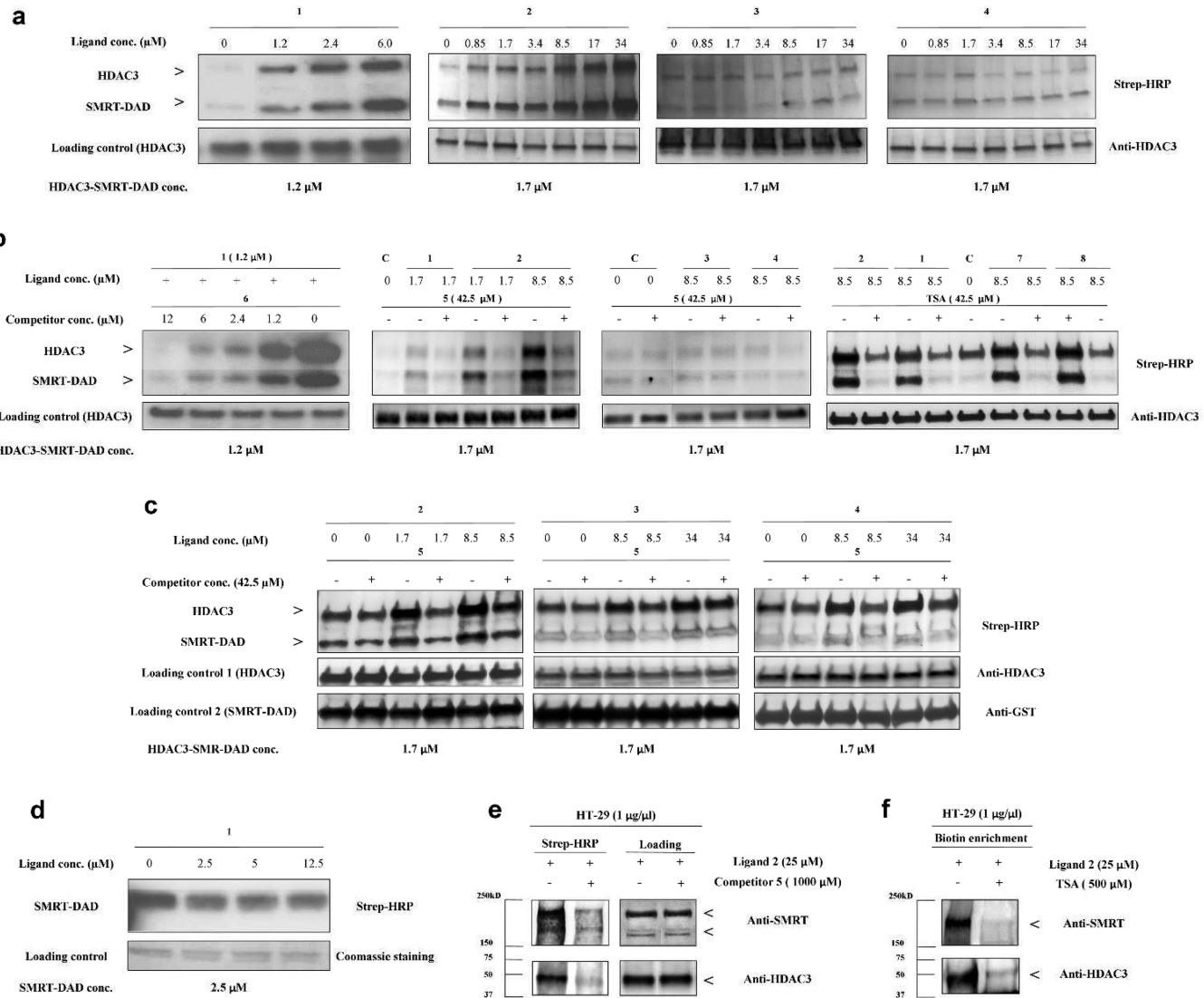


Figure 1.

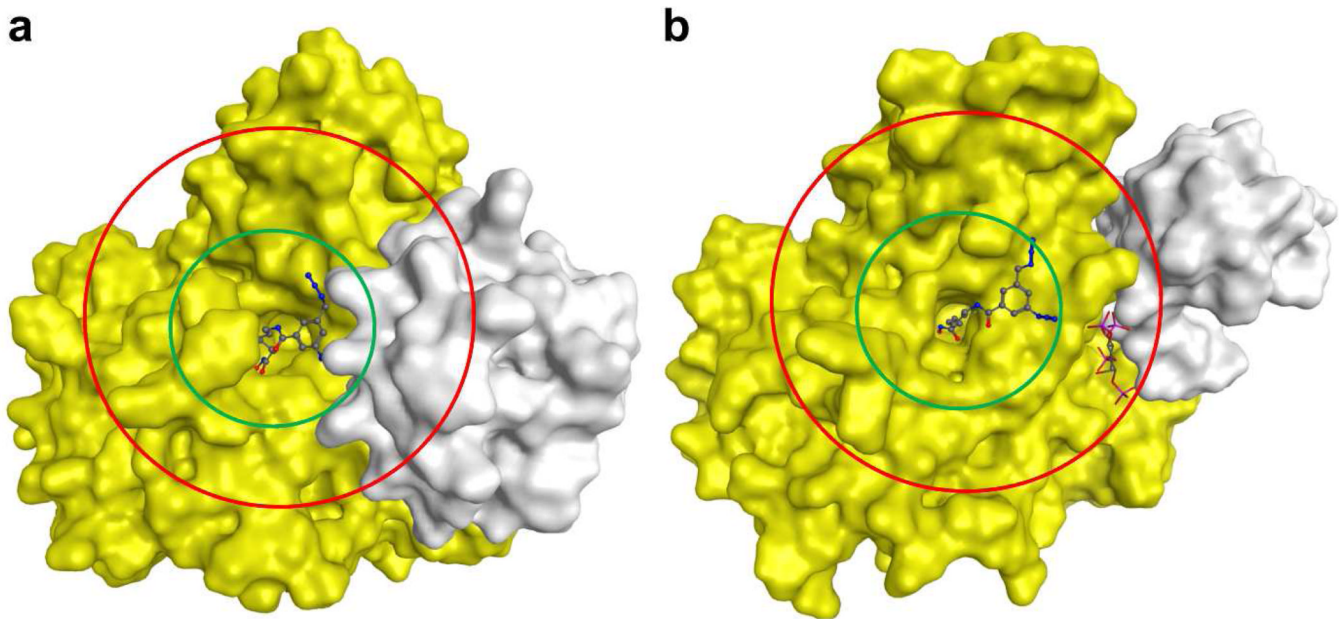
The chemical structures of the probes **1–8**, the alkyne biotin **9**, and TSA and IC₅₀ values of probes **1–8** and TSA against HDAC3-SMRT-DAD complex. IC₅₀ values are expressed as mean ± standard deviation of at least two independent experiments.



Scheme 1.
Synthesis of probes **2-5**^a

**Figure 2.**

Biotinylation levels of recombinant HDAC3-SMRT-DAD and cellular HDAC3-SMRT complex with probes **1-8**. (a) Photocrosslinking of probes **1-4** with recombinant HDAC3-SMRT-DAD. (b) Photocrosslinking of probes **1-8** in the presence of fixed concentration of monoazide probe **5** or TSA (42.5 μM) and varied concentration of probe **6** (1.2-12 μM). (c) Photocrosslinking of probes **2-4** under denaturing conditions (2% SDS) and a fixed concentration of probe **5**, followed by (3+2) cycloligation with tag **7**. (d) Photocrosslinking of probe **1** with SMRT-DAD only. (e) Soluble whole cell lysates from the colorectal cancer cell line HT-29 photocrosslinked with probe **2** (25 μM) in the presence or absence of monoazide probe **5** (1000 μM). (f) Same as e in the presence or absence of TSA (500 μM) followed by biotin enrichment on streptavidin beads. The biotinylated adducts were identified using streptavidin conjugated horseradish peroxidase (Strep-HRP) and protein bands were identified using antibodies of HDAC3 and SMRT, at a dilution factor of 1:4000 and 1:1000, respectively. The data is a representation of at least two independent experiments

**Figure 3.**

A comparison between the photolabeling based homology model and the X-ray structure of HDAC3-SMRT complex with regard of the interaction of SMRT-DAD and probe **2**. (a) HDAC3-SMRT-DAD complex constructed using the homology model and photolabeling analysis. The solvent accessible area of HDAC3 is rendered as yellow surface, SMRT-DAD – white. A representative pose of probe **2** is shown as ball-and-stick model. The maximum distance reached by the diazide portion of probes **1** and **2** is rendered as red and green circles, respectively. (b) Same as **a** based on the X-ray structure (PDB: 4A69).

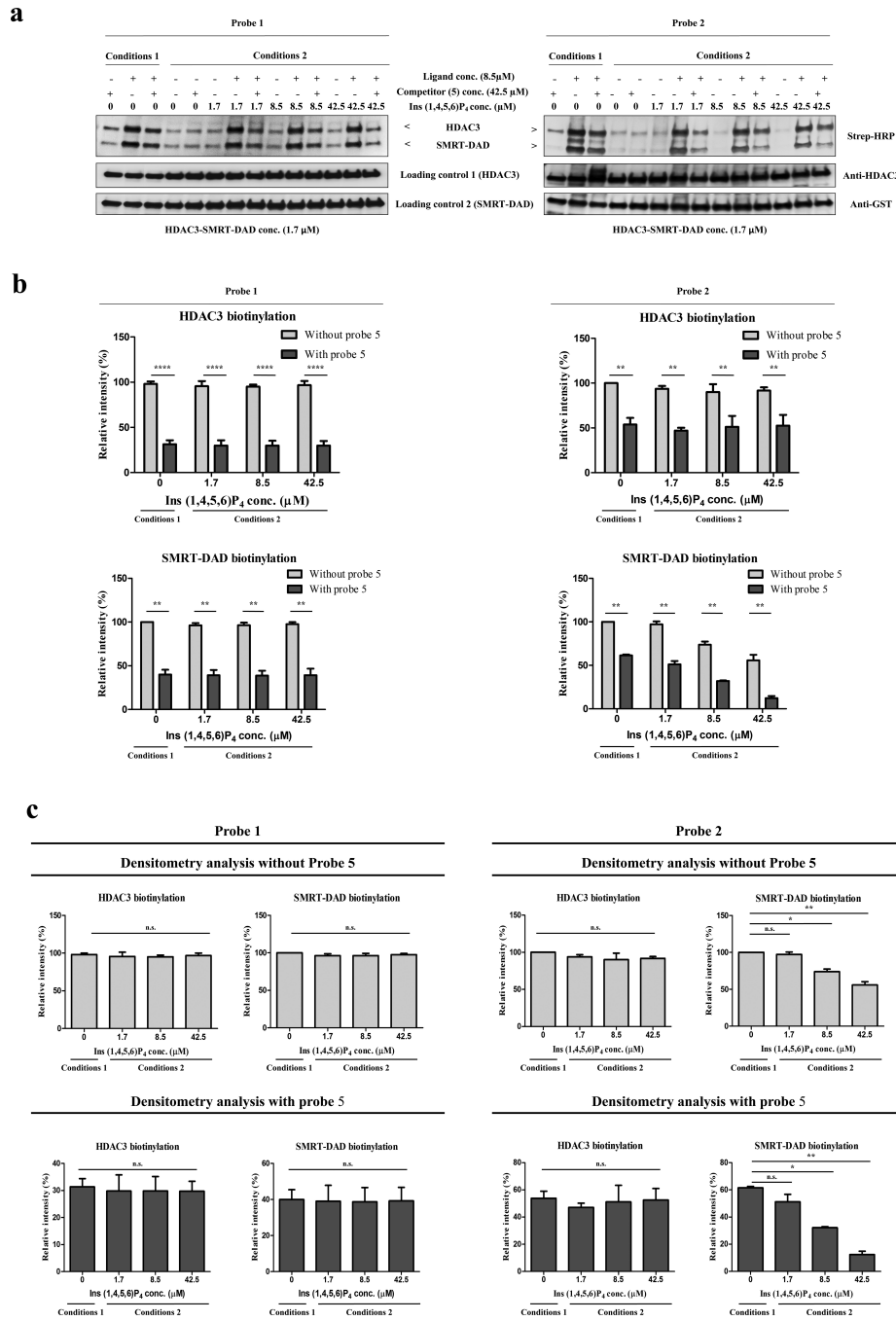


Figure 4.
The effect of Ins(1,4,5,6)P₄ on the photocrosslinking of probe **1** and **2** with HDAC3-SMRT-DAD complex. **(a)** Photocrosslinking of probe **1** and **2** (8.5 μ M) with HDAC3-SMRT-DAD, in the presence or absence of monoazide probe **5** (42.5 μ M) and in the presence of Ins(1,4,5,6)P₄ at three concentrations (1.7, 8.5, 42.5 μ M). Conditions 1 represent the in-house optimized conditions for photolabeling (25 mM Tris-HCl, adjusted pH=8, 25 mM NaCl, 2.7mM KCl, 1 mM MgCl₂, 0.1% triton X-100) and conditions 2 represent the pull down assay conditions from Schwabe et al paper⁽¹⁷⁾ (50 mM Tris-HCl, adjusted pH=7.5, 50 mM CH₃COOK, 5% glycerol, 0.3% triton X-100). **(b)** Densitometry analysis shows the

band density ratios of the biotinylation level of HDAC3 and SMRT-DAD to the loading of HDAC3 and SMRT-DAD at each concentration of Ins(1,4,5,6)P₄. Two-way ANOVA revealed a significant decrease in the biotinylation of HDAC3 and SMRT signal in the presence of monoazide probe **5** (**, $p < 0.01$) with a significant contribution of Ins(1,4,5,6)P₄ (***, $p < 0.001$) in further decrease of the biotinylation signal of SMRT only in the case of probe **2**. There was no significant interaction between the presence of probe **5** and Ins(1,4,5,6)P₄ (**c**) Densitometry analysis same as (**b**). One-way ANOVA revealed significant decrease in biotinylation of SMRT-DAD ,only in case of probe **2**, at two concentration (8.5 and 42.5 μ M) of Ins(1,4,5,6)P₄ (**, $p < 0.01$; *, $p < 0.05$), but no significant difference in the biotinylation of HDAC3 at any concentration of Ins(1,4,5,6)P₄ ($p < 0.336$) in the presence or absence of probe **5**. The data is plotted as the average of at least 2 independent experiments +/- SD.

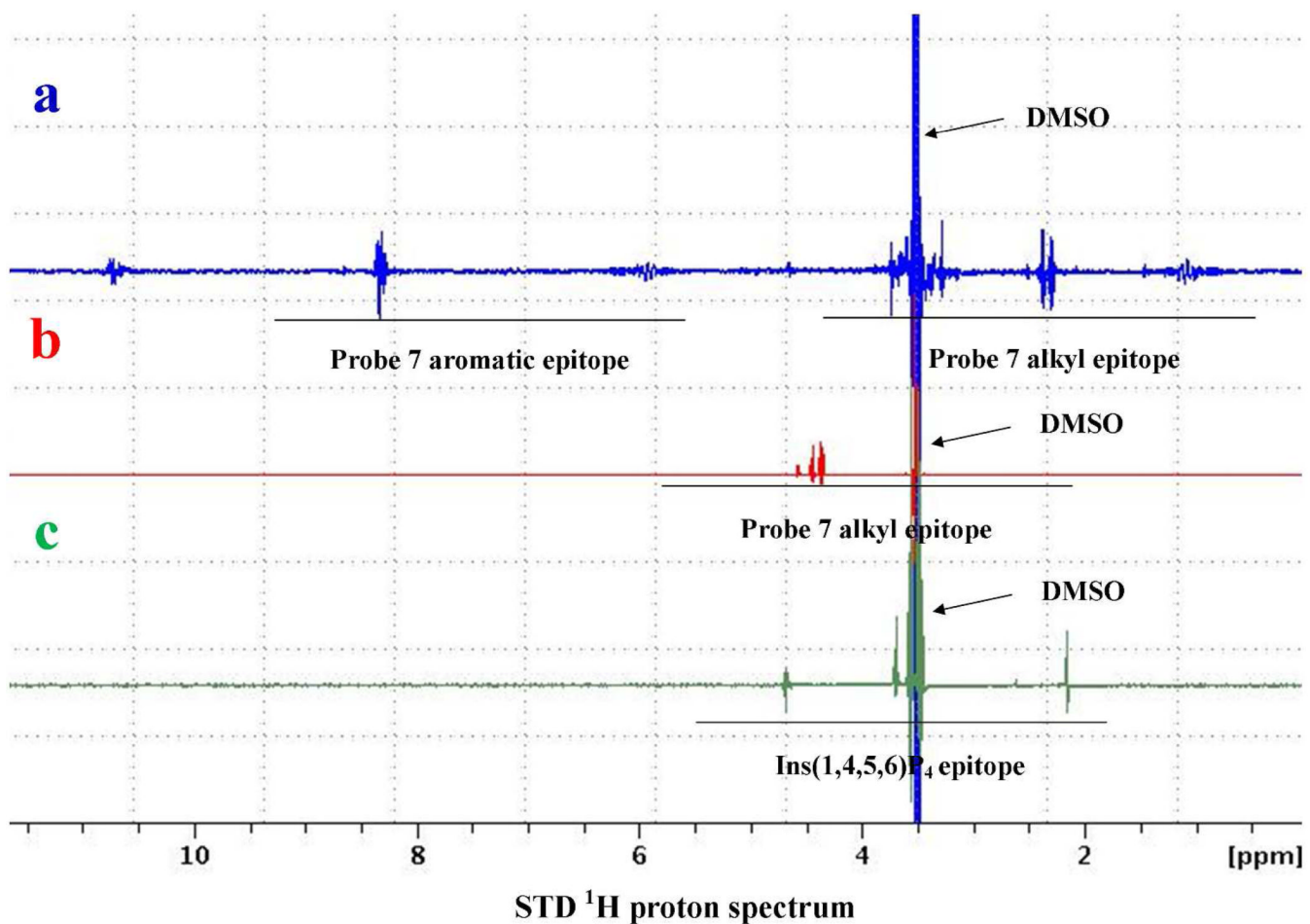
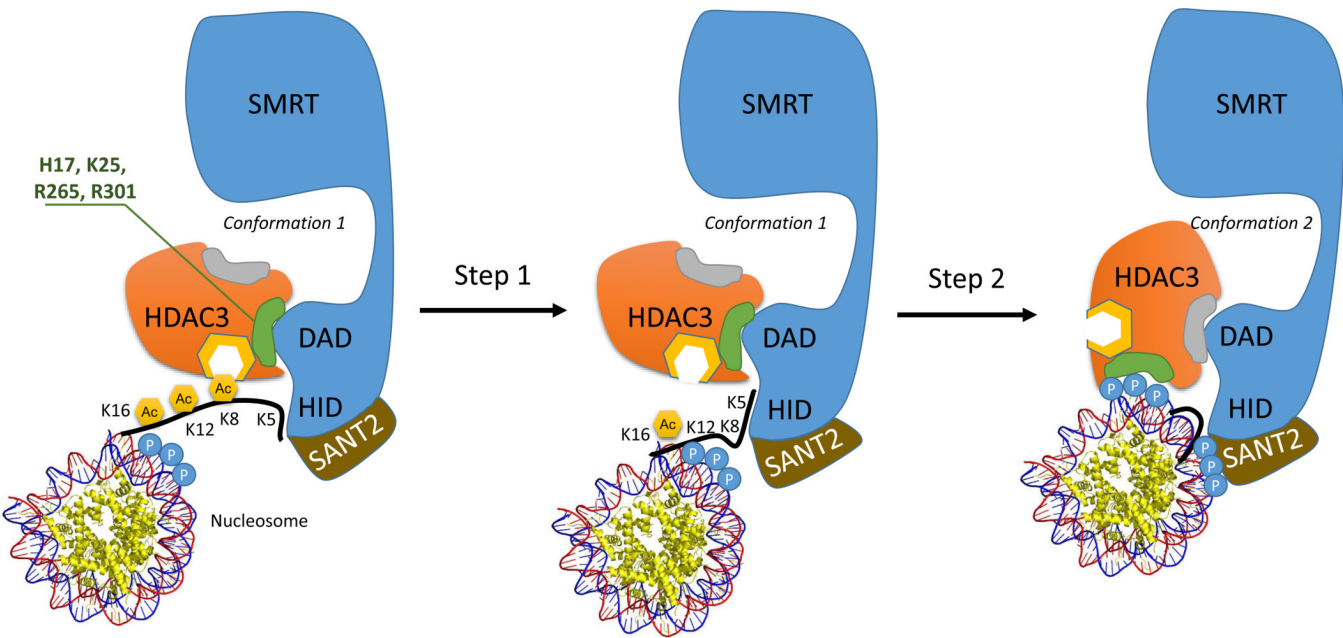


Figure 5.

Saturation transfer difference (STD) spectra of (a) 100 μM probe 7 with 1 μM HDAC3-SMRT-DAD complex without Ins(1,4,5,6) P_4 (blue), (b) same as a with 25 μM Ins(1,4,5,6) P_4 (red), (c) 1 μM HDAC3-SMRT-DAD complex with 25 μM Ins(1,4,5,6) P_4 (green). Signal assignments are marked on the spectra.

**Figure 6.**

Proposed regulatory role of the conformational switch in the HDAC3-SMRT complex. Step 1 - the feed forward model of histone deacetylation in *conformation 1*,⁽¹²⁾ step 2 – the conformational switch model where deacetylation of histone H4 is terminated by adopting *conformation 2*. The HDAC3-SMRT-DAD binding interfaces in *conformations 1* and *2* and the HDAC3 catalytic site are rendered by green, gray, and yellow, respectively. The histone tail, the acetylated lysine residues, and the phosphate groups on the deoxyribose sugars on the DNA are rendered by black line, yellow hexagons, and blue circles, respectively.